Int. J. Adv. Eng. Pure Sci. 2025, 37(3): <293-298>
DOI: 10.7240/jeps.1703374

**RESEARCH ARTICLE** / ARAŞTIRMA MAKALESİ

# Evaluation of biomaterial containing alginate and egg-shell membrane incorporated with β-tricalcium phosphate for treatment of bone defects

**Semra UNAL** [1,2]

[1] *Genetic and Metabolic Diseases Research and Investigation Center, Marmara University, Istanbul, Turkey*

[2] *Institute of Neurological Sciences, Marmara University, Istanbul, Turkey*

**Abstract**

The freeze-drying procedure was used to create the scaffold that was meant to cure bone deformities. Fourier transform infrared (FTIR) spectroscopy, X-ray diffraction analysis, swelling and degradation ratio, and scanning electron microscopy (SEM) tests were used to characterize the scaffolds. Osteoblast cells were used in an in vitro cytotoxicity test to evaluate the scaffolds' biocompatibility. The results of the characterization revealed an interconnected porous structure and significant ionic connections between the alginate, egg-shell membrane, and β-tricalcium phosphate (β-TCP). The scaffolds are regarded as nontoxic because the cell viability was more than 80%. When all the findings are evaluated, β-TCP with alginate/egg-shell membrane can be regarded as appropriate for bone treatment applications.

**Keywords:** alginate, egg shell membrane, beta-tricalcium phosphate, tissue engineering

## I. INTRODUCTION

Biomaterials utilized in tissue engineering that emulate the physicochemical features of the native extracellular matrix (ECM) have been demonstrated to support cellular adhesion, proliferation, migration, and new tissue formation. The structure of natural bone is a complex composite, consisting of hydroxyapatite (HA) crystals organized within an organic matrix primarily composed of type I collagen (Col) [1]. According to the current state-of-the-art, it is compatible with the combination of different materials, inorganic and organic, as well as the immediate incorporation of cells to accelerate the bone regeneration process [2]. The three-dimensional (3D) composite systems developed in recent studies aim to replicate the structural and biochemical characteristics of bone ECM—comprising a mineral phase mainly of calcium phosphate, typically in the form of HA, and a fibrous organic matrix rich in type I collagen [3]. To achieve this, the researchers combine ceramics with advanced mechanical properties such as hydroxyapatite, tricalcium phosphate (TCP) and glass ceramics with highly bioactive and biocompatible polymers such as collagen, alginate, chitosan and gelatin to create matrices that support bone tissue formation. [4]. Eggshell membrane (ESM), being a rich source of collagen, glycosaminoglycans, chondroitin sulfate, and hyaluronic acid, is considered a promising candidate for biomedical applications in tissue engineering [5–7]. These components closely resemble those found in bone's natural collagenous matrix, positioning ESM as a suitable structural base for scaffold fabrication. Eggshell, one of the approximately 5 million tons of high-value biological resources produced annually in industry and households, is ignored and generally discarded as waste [8]. It is important to consider the cost-effectiveness of a biomaterial that can reduce the economic burden of high-priced biomedical materials. ESM can therefore be considered as a cost-reducing natural material alternative. Sodium alginate, a hydrophilic, biocompatible polysaccharide extracted from brown algae, is well-known for its gel-forming ability and high viscosity in aqueous environments [2]. Composite biomaterials combining alginate with inorganic fillers have been effectively employed to mimic the microenvironment of bone [9]. In this context, incorporating β-tricalcium phosphate into alginate/ESM-based biopolymers may further enhance their regenerative capacity in treating bone defects. Furthermore, innovations in fabrication techniques could improve the performance of such scaffolds in bone tissue engineering applications. Thus, a hybrid scaffold composed of alginate, β-TCP, and ESM is anticipated to offer an effective platform for *in vitro* osteoblast culture. The objective of this study is to synthesize and characterize scaffolds composed of alginate, egg shell membrane, and β-TCP for tissue engineering applications. To the best of our knowledge, this

**Corresponding Author:** SEMRA UNAL, **Tel:** 0539 722 45 45, **E-mail:** semra.unal@marmara.edu.tr

**Submitted:** 24.05.2025, **Revised:** 12.07.2025, **Accepted:** 05.08.2025

novel ternary system has not been previously explored for cell proliferation. In this study, swelling and degradation properties and assessment of cell proliferation activity of cells on designed material have been carried out.

## II. MATERIALS AND METHODS

### 2.1. Fabrication of ALG/ESM/TCP scaffolds

Fresh eggs separated from yolk and albumen were obtained from a local restaurant and then rinsed with sterile distilled water followed by disinfected with ethanol. The eggshells were kept in 2% (v/v) acetic acid solution for 1 hour and the ESM were carefully peeled off from eggshells with forceps. Following this, the ECM was subjected to freeze-drying until completely dried. Different types of ALG/ESM/TCP were prepared by 100 mL of ALG (5 wt.%) aqueous solution with various amounts of β-TCP (0, 1, 2.5 wt.%) in the presence of ESM (100 mg). Freeze drying method was used in the production of ALG/ESM/TCP scaffolds. The prepared ALG/ESM/TCP solutions were poured into 24-well plates and treated with 5% $CaCl_2$ solution overnight. Post-crosslinking, the constructs were extensively washed with double-distilled water to remove residual calcium ions and then freeze-dried at –50 °C for 24 hours. The similar procedure was used to prepare the control ALG/ESM scaffold.

### 2.2. Characterization of ALG/ESM/TCP scaffolds

Chemical analyses of crosslinking of ALG/ESM and ALG/ESM/TCP scaffolds was verified via the Fourier transform infrared (FTIR) spectrometer (model 4600 Jasco, Japan). The analysis was performed within the wavelength range 400–4000 $cm^{-1}$. All spectra were baseline-corrected and calibrated to ambient atmospheric conditions. The morphology of the control ALG/ESM and ALG/ESM/TCP scaffolds was analyzed by the Scanning Electron Microscopy (SEM, EVO MA-10, Zeiss, Germany) after sputter-coating with gold at an accelerating voltage of 10 kV. The crystalline structures of the nanocomposites was analyzed by X-ray diffraction (XRD, Shimadzu-6100, Japan) using Cu Kα radiation (λ = 1.54060 A°). The scan range was changed from 10° to 40°, and the scan speed was altered to 2° min−1.)

### 2.3. Swelling studies

ALG/ESM and ALG/ESM/TCP scaffolds were allowed to swell in phosphate buffered saline (PBS; pH 7.4) at 37 °C to determine their swelling behavior. At the beginning of each experiment, the dried scaffolds were weighed accurately to determine Wd. The swollen samples were removed from PBS at predetermined intervals over a period of 120 hours, excess surface liquid was removed with filter paper and reweighed to determine the swollen weight (Ww). PBS was replaced by fresh PBS each time. Triplicate measurements were taken for each data point. Swelling ratio was calculated using the formula (1).

$$Swelling\ degree = [(Ww - Wd)/Wd] \times 100 \quad \textbf{(1)}$$

### 2.4. In vitro degradation analysis

Scaffold degradation profiles were monitored over 4 weeks in PBS at 37 °C. Samples with known initial weight (Wi) were incubated in 10 mL PBS and retrieved at set intervals. Each specimen was washed with distilled water, freeze-dried, and reweighed to obtain the final weight (Wf). Weight loss percentage was determined using the formula (2):

$$Weight\ loss(\%) = [(Wi - Wf)/Wi] \times 100 \quad \textbf{(2)}$$

### 2.5. In vitro biocompatibility analysis

Biocompatibility analysis of the samples was assessed using the 3-(4,5-dimethylthiazol-2-yl)-2,5-diphenyl tetrazolium bromide (MTT) assay on human osteoblast cells (ATCC hFOB 1.19 CRL-3602™). Cells were cultured in DMEM medium enriched with 10% fetal bovine serum and 1% penicillin/streptomycin. Disc-shaped scaffolds (16 mm diameter) were sterilized using UV light for 2 hours before being seeded with $1\times10^5$ cells per well in 24-well plates. Control groups included cells cultured on standard tissue culture plastic (2D). After incubation periods of 1, 4, and 7 days, the culture medium was removed, and wells were rinsed with PBS (pH 7.4). MTT solution (0.5 mg/mL) was added to each well and incubated at 37 °C for 4 hours. The resulting formazan crystals were dissolved in 1 mL of dimethyl sulfoxide (DMSO), and absorbance was measured at 590 nm using a microplate reader.

## III. RESULTS AND DISCUSSION

The initial mixing of β-tricalcium phosphate (β-TCP) with alginate solution under ambient conditions led to a partial scaffold formation, observed visually as a weak hydrogel. This early-stage network formation is likely initiated by ionic interactions between the divalent calcium ions ($Ca^{2+}$) on the surface of β-TCP particles and the carboxylate groups of alginate [10]. To enhance scaffold integrity, $CaCl_2$ solution was added, promoting a complete ion-exchange where $Ca^{2+}$ replaced Na+ ions in the alginate matrix, resulting in a fully crosslinked structure. The final composite scaffolds were obtained by freeze-drying the crosslinked gels at -50°C for 24 hours.

Fourier-transform infrared (FTIR) spectroscopy revealed characteristic peaks confirming the presence of scaffold components. ALG-ESM, ALG-ESM-TCP1 and ALG-ESM-TCP2.5 samples were freeze-dried. FTIR spectra of freeze-dried ALG-ESM, ALG-ESM-TCP1 and ALG-ESM-TCP2.5 samples are shown in Fig. 1. Most of the peaks in the sample spectrum appeared to come from its components. The sharp peaks at 551 $cm^{-1}$ and 605 $cm^{-1}$ were attributed to phosphate group ($PO4^{3-}$) in β-TCP [10]. ESM has a high density of functional groups, such as amines, amides, and carboxylic acids, and strong chemical stability. Covalent cross-links are created between the carboxyl groups on the alginate chains and the amine groups on the ESM particles. Furthemore, a peak at 1411 $cm^{-1}$ and 1601 $cm^{-1}$ for related stretching vibrations of COO− indicates the presence of carboxylate groups on alginate in the scaffold samples, showing that functional groups were well maintained [2]. The C-O stretching vibrations are represented by the absorption peak at 1156 $cm^{-1}$ [11]. O–H and N–H stretching bonds are represented by the large peak at about 3320 $cm^{-1}$ [11,12]. In addition, the typical ESM bonds are observed in the same spectrum as well.

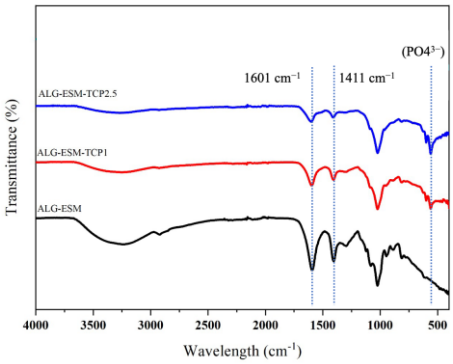


**Figure 1:** FTIR spectra of ALG-ESM, ALG-ESM-TCP1 and ALG-ESM-TCP2.5 scaffolds.

In Figure 2, the patterns seen at 2θ values of 25.8° (1010) and 32.5° (0210) validated the crystalline structure of the β-TCP sample. All of the scaffold samples' reflection patterns showed up at the same 2θ angles as the β-TCP sample, confirming that the scaffold materials successfully integrated β-TCP. The composite spectrums are observed to be amorphous in nature due to high concentration of sodium alginate–egg shell membrane matrix with crystalline β-TCP.

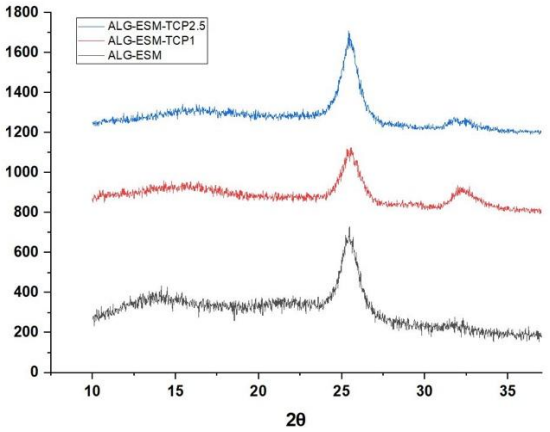


**Figure 2:** X-ray diffraction (XRD) patterns of ALG-ESM, ALG-ESM-TCP1 and ALG-ESM-TCP2.5 scaffolds.

The cross-sectional surface morphology of freeze-dried ALG-ESM, ALG-ESM-TCP1, and ALG-ESM-TCP2.5 samples was examined using SEM, as shown in Fig. 3. In ALG-ESM-TCP1 and ALG-ESM-TCP2.5 scaffolds, β-TCP is easily seen. While the ESM fiber structure was clearly seen in ALG-ESM, ALG-ESM-TCP1 scaffolds, it was observed that β-TCP particles were integrated into the fibers and covered the surface in ALG-ESM-TCP2.5 scaffold. As can be seen in Figure 5, samples formed complete pore structures and exhibit interconnection pores. Among the samples, the ALG-ESM-TCP2.5 scaffold exhibited the most pronounced porous structure, with more evenly distributed large, prominent pores and thicker pore walls, indicating a stronger overall structure. These features were more clearly visible at 200X magnification. Furthermore, at 1000X magnification, crystalline β-TCP was observed in both scaffold systems, confirming the successful incorporation of β-TCP into the scaffolds. The porous structure plays a crucial role in biomedical applications for cellular adhesion, intercellular communication, and oxygen and nutrient transfer. Composite scaffolds with uniform pore architectures are preferred over those with non-uniform pores in biomedical applications. Although tissue growth on scaffolds with irregular pore sizes may lead to poor biomechanical qualities, cell attachment can occur on heterogeneous scaffolds [10].

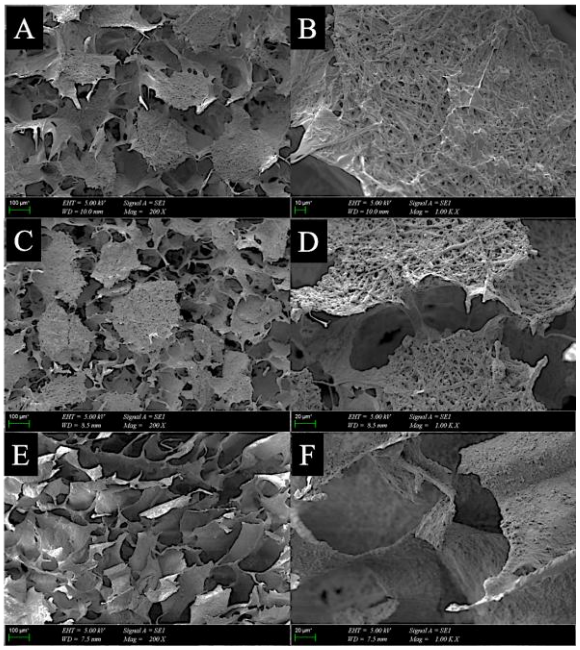


**Figure 3:** SEM images of ALG-ESM (A, B), ALG-ESM-TCP1 (C, D ) and ALG-ESM-TCP2.5 (E, F) scaffold.

The equilibrium swelling behavior of different ALG-ESM scaffold samples was analyzed and the results are presented in Fig. 4. The samples were weighed at various time points—1, 6, 12, 24, 48, 72, 96, and 120 hours—after being immersed in PBS solution at 37°C. All samples began to swell after 1 hour of incubation. The results showed that the degree of swelling was generally higher in samples with greater ALG-ESM-TCP1 content throughout most time points. The highest swelling degrees were observed at 72 hours, with the ALG-ESM, ALG-ESM-TCP1, and ALG-ESM-TCP2.5 samples reaching swelling values of 218.05 ± 17.01%, 283.61 ± 19.96%, and 255.52 ± 12.96%, respectively. Between 72 and 120 hours, the swelling rate slowed and became more stable.

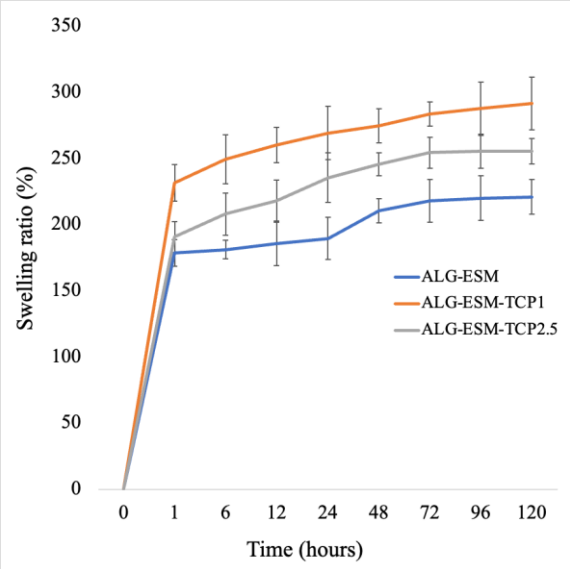


**Figure 4:** Swelling ratio of ALG-ESM, ALG-ESM-TCP1 and ALG-ESM-TCP2.5 scaffolds according to incubation time.

The degradation kinetics for all scaffold samples were monitored for 4 weeks under simulated physiological conditions at 37 °C and the calculated weight retention percentages are shown in Fig. 5. From the start of the experiment to day 7, the ALG-ESM, ALG-ESM-TCP1, and ALG-ESM-TCP2.5 samples degraded by 70.37 ± 6.52%, 70.16 ± 7.71%, and 52.59 ± 8.24%, respectively. During weeks 1 to 3, the degradation rates slowed, with all samples retaining up to 30% of their original mass. After week 3, the degradation ratio increased and ALG-ESM, ALG-ESM-TCP1 and ALG-ESM-TCP2.5 were calculated the degradation ratio 84.93 ± 8.59%, 89.07 ± 2.38% and 89.63 ± 2.79%, respectively. After 4 weeks of incubation, the form of all scaffold samples degraded entirely.

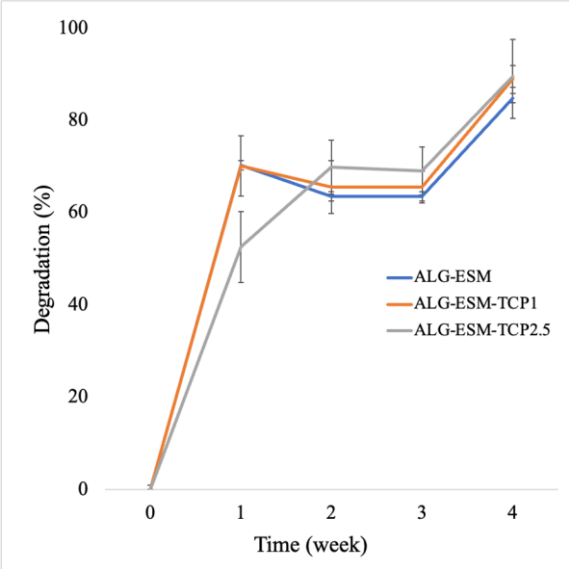


**Figure 5.** Degradation ratio of ALG-ESM, ALG-ESM-TCP1 and ALG-ESM-TCP2.5 scaffolds according to incubation time.

While the scaffolds used in this study exhibited a relatively rapid degradation profile, which may be advantageous for short-term applications in bone regeneration, their degradation rate was found to be faster than the typical healing time required for bone defects, which may extend up to 6 months. The complete degradation of the scaffolds within 4 weeks raises concerns about their ability to provide sufficient support during the crucial initial stages of bone healing. Several strategies could be employed to extend the degradation time of these scaffolds, including increasing the crosslinking density, incorporating biodegradable polymers with slower degradation rates, and modifying the scaffold's structural properties.

The MTT assay was employed to assess the cytotoxicity of ALG-ESM scaffold samples on human osteoblast cells, with comparison to the control (2D). In the control group, cells were cultured in the culture medium, while in the experimental group, cells were cultured on the scaffold samples. The cell viability rates of the scaffold samples, compared to the control, are shown in Fig. 6. All samples exhibited cell viability exceeding 80% for both β-TCP concentrations in the hydrogels, indicating that they are non-cytotoxic and biocompatible. In all samples, the viability of human osteoblast cells increased with β-TCP concentration at day 1 incubation with 87.3 ± 1.09%, 93.7 ± 1.72% and 95.4 ± 1.35% in ALG-ESM, ALG-ESM-TCP1 and ALG-ESM-TCP2.5, respectively. On day 4 and day 7 of cell incubation, ALG-ESM-TCP1 showed cell viability above 100%, which is competitive with the control group. *In vitro* biological response of β-TCP-based scaffolds was studied using osteoblast [13] and fibroblast cells [14,15] to analyze the biocompatibility of materials for orthopedic applications. Algul et al. [14] noticed that the alginate and chitosan layer with the highest β-TCP concentration (70 wt%) among the samples led to higher cell viability, highlighting the properties of calcium phosphates to facilitate cellular adhesion and promote cellular proliferation. At 7 day of cell incubation in the study, β-TCP content increased the percentage of cell viability. In addition to higher cell viability, they emphasized the ability of calcium phosphates to facilitate cellular adhesion and promote cellular proliferation.

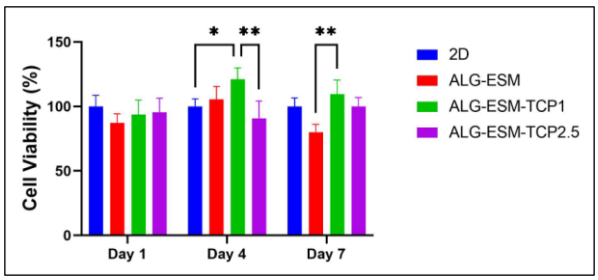


**Figure 6:** Viability of human osteoblast cells on the ALG-ESM, ALG-ESM-TCP1 and ALG-ESM-TCP2.5 scaffolds after 1, 4, and 7 days of incubation period. Statistical analysis were done in comparison to the two-dimensional (2D) monolayer culture by one-way ANOVA (*p<0,05, **p<0,01) Turkey-Kramer Multiple Comparisons Test.

## IV. CONCLUSION

In this study, scaffolds based on ALG-ESM, ALG-ESM-TCP1, and ALG-ESM-TCP2.5 were prepared using a freeze-drying method. The formation of Schiff's base linkages was confirmed by FTIR analysis, which also demonstrated the successful integration of β-TCP into the scaffold. The concentration of β-TCP influenced the scaffold formation, characteristics, and *in vitro* cytocompatibility. Overall, the scaffolds were porous, biodegradable, biocompatible, and non-cytotoxic. Among the samples, the ALG-ESM-TCP1 scaffold exhibited the most favorable results, including rapid gelation time, an interconnected porous structure with the highest porosity, acceptable swelling capacity, and excellent in vitro cytocompatibility. These findings highlight its potential for supporting, repairing, and regenerating non-displaced or non-load-bearing bone injuries. In order to overcome some limitations of our investigation, the degradation rate could be better aligned with the healing process, ensuring that the scaffold provides sustained support while promoting successful bone regeneration. Future study will aim to explore these approaches to improve the performance and applicability of the scaffolds for long-term bone tissue engineering applications.

## REFERENCES


**[1]** Cakmak, A.M., Unal, S., Sahin, A., Oktar, F.N., Sengor, M., Ekren, N., Gunduz, O., & Kalaskar, D.M. (2020). 3D printed polycaprolactone/gelatin/bacterial cellulose/hydroxyapatite composite scaffold for bone tissue engineering. *Polymers (Basel)*, 12, 1–14. doi:10.3390/polym12091962.

**[2]** Silva-Barroso, A.S., Cabral, C.S.D., Ferreira, P., Moreira, A.F., & Correia, I.J. (2023). Lignin-enriched tricalcium phosphate/sodium alginate 3D scaffolds for application in bone tissue regeneration. *International Journal of Biological Macromolecules*, 239. doi:10.1016/j.ijbiomac.2023.124258.

**[3]** Lin, X., Patil, S., Gao, Y.G., & Qian, A. (2020). The Bone Extracellular Matrix in Bone Formation and Regeneration. *Frontiers in Pharmacology*, 11, 1–15. doi:10.3389/fphar.2020.00757.

**[4]** Garimella, A., Ghosh, S.B., & Bandyopadhyay-Ghosh, S. (2024). Biomaterials for bone tissue engineering: achievements to date and future directions. *Biomedical Materials*, 20. doi:10.1088/1748-605X/ad967c.

**[5]** Jia, J., Duan, Y.Y., Yu, J., & Lu, J.W. (2008). Preparation and immobilization of soluble eggshell membrane protein on the electrospun nanofibers to enhance cell adhesion and growth. *Journal of Biomedical Materials Research - Part A*, 86, 364–373. doi:10.1002/jbm.a.31606.

**[6]** Farjah, G.H., Mohammdzadeh, S., & Javanmard, M.Z. (2020). The effect of lycopene in egg shell membrane guidance channel on sciatic nerve regeneration in rats. *Iranian Journal of Basic Medical Sciences*, 23, 527–533. doi:10.22038/ijbms.2020.40228.9525.

**[7]** Adali, T., Kalkan, R., & Karimizarandi, L. (2019). The chondrocyte cell proliferation of a chitosan/silk fibroin/egg shell membrane hydrogels. *International Journal of Biological Macromolecules*, 124, 541–547. doi:10.1016/j.ijbiomac.2018.11.226.

**[8]** Li, X., Cai, Z., Ahn, D.U., & Huang, X. (2019). Development of an antibacterial nanobiomaterial for wound-care based on the absorption of AgNPs on the eggshell membrane. *Colloids and Surfaces B: Biointerfaces*, 183, 110449. doi:10.1016/j.colsurfb.2019.110449.

**[9]** Ocando, C., Dinescu, S., Samoila, I., Ghitulica, C.D., Cucuruz, A., Costache, M., & Averous, L. (2021). Fabrication and properties of alginate-hydroxyapatite biocomposites as efficient biomaterials for bone regeneration. *European Polymer Journal*, 151, 110444. doi:10.1016/j.eurpolymj.2021.110444.

**[10]** Afriani, F., Dahlan, K., Nikmatin, S., & Zuas, O. (2015). Alginate Affecting The Characteristics Of Porous Beta-Tcp/Alginate Composite Scaffolds. *Journal of Optoelectronics and Biomedical Materials*. https://publons.com/publon/31759775/.

**[11]** Liang, L., Hou, T., Ouyang, Q., Xie, L., Zhong, S., Li, P., Li, S., & Li, C. (2020). Antimicrobial sodium alginate dressing immobilized with polydopamine-silver composite nanospheres. *Composites Part B: Engineering*, 188, 107877. doi:10.1016/j.compositesb.2020.107877.

**[12]** Mohammadzadeh, L., Rahbarghazi, R., Salehi, R., & Mahkam, M. (2019). A novel egg-shell membrane based hybrid nanofibrous scaffold for cutaneous tissue engineering. *Journal of Biological Engineering*, 13, 1–15. doi:10.1186/s13036-019-0208-x.

**[13]** Guler, E., Baripoglu, Y.E., Alenezi, H., Arikan, A., Babazade, R., Unal, S., Duruksu, G., Alfares, F.S., Yazir, Y., Oktar, F.N., Gunduz, O., Edirisinghe, M., & Cam, M.E. (2021). Vitamin D3/vitamin K2/magnesium-loaded polylactic acid/tricalcium phosphate/polycaprolactone composite nanofibers demonstrated osteoinductive effect by increasing Runx2 via Wnt/B-catenin pathway. *International Journal of Biological Macromolecules*. doi:10.1016/j.ijbiomac.2021.08.196.

**[14]** Algul, D., Sipahi, H., Aydin, A., Kelleci, F., Ozdatli, S., & Yener, F.G. (2015). Biocompatibility of biomimetic multilayered alginate-chitosan/β-TCP scaffold for osteochondral tissue. *International Journal of Biological Macromolecules*, 79, 363–369. doi:10.1016/j.ijbiomac.2015.05.005.

**[15]** Ghaffari, R., Salimi-Kenari, H., Fahimipour, F., Rabiee, S.M., Adeli, H., & Dashtimoghadam, E. (2020). Fabrication and characterization of dextran/nanocrystalline β-tricalcium phosphate nanocomposite hydrogel scaffolds. *International Journal of Biological Macromolecules*, 148, 434–448. doi:10.1016/j.ijbiomac.2020.01.112.